AD-A139 067 RF PROPERTIES OF SUPERCONDUCTING A-15 COMPOUNDS(U) 1/1
STANFORD UNIV CA EDWARD L GINZTON LAB OF PHYSICS
M R BEASLEY ET AL. DEC 83 GL-3675 N00019-82-C-0286
UNCLASSIFIED F/G 20/3 NL

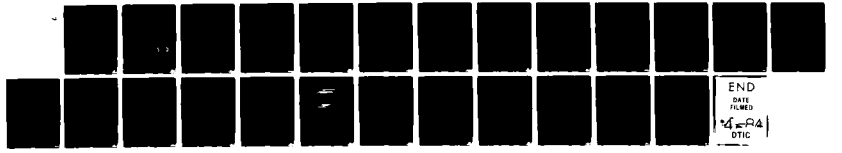

END
DATE FILMED
4-84
DTIC

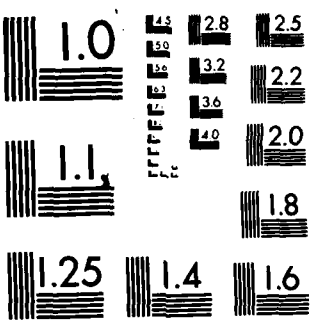

(12)

AD A139067

RF PROPERTIES OF SUPERCONDUCTING A-15 COMPOUNDS

Final Technical Report

for the period

15 June 1982 - 14 June 1983

N00019-82-C-0286

Principal Investigators

M.R. Beasley and H.A. Schwettman

G.L. Report No. 3675

December 1983

Edward L. Ginzton Laboratory
W.W. Hansen Laboratories of Physics
Stanford University
Stanford, California 94305

Contract N00019-82-C-0286

Final Technical Report

for the period

15 June 1982 - 14 June 1983

I. INTRODUCTION

The extremely low surface resistance exhibited by superconductors makes possible some interesting and important applications in microwave electronics. Chief among these are (1) the use of high-field superconducting cavities as high-power, coherent, pulsed, microwave sources and(2) the use of low-loss, low-dispersion rf striplines as communication links or delay elements in high-speed digital and analog signal processing circuits. The specific interests of this contract were the former. For these applications the most promising superconductors are those with a high transition temperature (high T_c), since they have the best potential performance characteristics (lowest losses and highest magnetic field breakdown). In addition, because of their higher operating temperature, these superconductors may be interfaced with small cryogenic refrigerators. The primary objective of this program has been to study the rf properties of the high-T_c, A15 superconductors [e.g., Nb_3Sn ($T_c \approx 18K$) and V_3Si($T_c \approx 15K$)], and in particular, to establish their rf superconducting characteristics and the relationship between these characteristics and their material properties. Because of the flexibility afforded to material studies, the samples have been prepared in thin-film form using vapor deposition.

Our work has concentrated on Nb_3Sn, an A15 material with the presumed advantage that its metallurgical characteristics were well understood.

Unfortunately, this has not been the case. We have measured the temperature dependence of the surface resistance of this material as a function of composition, deposition conditions, and (with some uncertainty) substrate temperature and compared our results with theoretical predictions. Our early samples (studied under preceding contracts) had broad rf superconducting transitions that we attributed to material inhomogeneities. Although some inhomogeneities have been eliminated, others appear to be intrinsic to the material. This observation is inconsistent with the accepted phase diagram. These problems have made it difficult so far to make homogeneous, single-phase, A15 films. Under the present contract we have examined some equilibrium two-phase samples from which we extracted the intrinsic surface resistance of the A15 phase alone. Thus we have established that single-phase A15 material has the expected theoretical behavior. Also, we are proposing a tentative new phase diagram for the Nb-Sn system which can explain our results. The implications of the new phase diagram for the preparation of homogeneous, single-phase, A15 Nb_3Sn will be discussed. Finally, we have developed a new approach to making homogeneous Nb_3Sn by a non-equilibrium film growth procedure. Preliminary results are reported here and are sufficiently promising that the prognosis for obtaining Nb_3Sn thin films with good rf properties appears favorable.

II. EXPERIMENTAL APPROACH

In earlier reports we have described our rf loss measurement apparatus, our measurement procedures, and the tests undertaken to confirm the validity of our measurements.[4,5,6] Here, only the materials studies are presented.

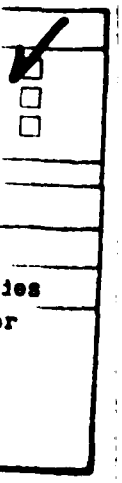

To establish the relationship between the rf losses of Nb_3Sn and its material properties, our approach has been to make samples in different portions of the phase diagram using various deposition conditions. In particular, the substrate temperature during film deposition (T_s), both its absolute value and its uniformity, has proved to be the most crucial factor in obtaining satisfactory material. Comparing the observed rf loss data with theoretical predictions and with each other has led to the unexpected conclusions about the Nb-Sn phase diagram referred to above.

III. EXPERIMENTAL RESULTS

We began our study of Nb_3Sn on the basis of the phase diagram[7] shown in Fig. 1. The positions of the representative samples discussed in this report are indicated, and their important preparation and material characteristics are listed in Table I. Figure 2 illustrates the evolution of the substrate holders used in making these samples, and Figs. 3-6 show the measured surface resistances as a function of temperature.

Note that the samples are identified by their evaporation number. When two samples were made simultaneously, the two samples are further distinguished by whether they were Nb rich (Nb^+) or Sn rich (Sn^+). (See positions on phase diagram, Fig. 1.)

To understand the significance of our results we must consider the Nb-Sn phase diagram (Fig. 1). Material made in the single-phase A15 region will have the lowest rf losses. Our samples are made in the region from 750-1,000°C and within ± 3% of stoichiometric Nb_3Sn which has a 25% Sn composition.

We are interested in the A15 region of the phase diagram from 700-1000°C. Below ~ 700°C, the material is sufficiently disordered that T_c is depressed. Above 1000°C, Sn re-evaporates, resulting in a Sn-poor low-T_c material. The single-phase A15 region is from 18-25% Sn, and the best superconducting properties were known to arise at stiochiometry (i.e., 25% Sn). At Sn concentrations below the A15 phase region a 2-phase region exists containing both the A15 phase and a lower-T_c, superconducting, BCC phase consisting of a Nb-Sn solid solution. To the right of the A15 phase is another 2-phase region comprising of a normal metal (Nb_6Sn_5) phase as well as the A15 phase. Samples made in the single-phase region of the diagram should be homogeneous, while those made in a two-phase region should not be. However, the degree to which the anticipated phase separation comes about depends on the strength of thermodynamic driving forces and the ease of diffusion.

To illustrate the nature of the materials problems in making Nb_3Sn, it is convenient to discuss our samples in chronological order.

A. Early Results

Our first Nb_3Sn sample G-80-122, (Fig. 3) is a good example of the presence of macro inhomogeneities. Compare the structure of the multiple transitions in G-80-122 with the single transition at T_c of the theoretical curve. We attribute macro inhomogeneities to gross temperature variations across the sample during deposition, due to inadequate anchoring of substrates to the substrate holder. G-80-122 was made using the Mark-I substrate holder [see Fig. 2(a)] in which the substrate was only loosely held at each end. This is clearly not good enough. To correct this deficiency, a Mark II substrate holder [Fig. 2(b)] was developed which pressed the substrate tightly to it, still, however, only at each end. Samples G-82-68 (Fig. 4) and

G-82-119 (Fig. 5) were made with this holder. Comparing their $R_s(T)$ curves with G-80-122, we see the multiple transitions have been eliminated. The problem of macro inhomogeneities is under control.

Unfortunately the transition for samples made in the nominally single-phase region, G-81-68 Nb^+ and G-81-119 Nb^+, are still too broad. By contrast the sample made in the two-phase (A15 and Nb_6Sn_5) region, G-81-119 Sn^+ shows a sharp transition but a large residual surface resistance. We can understand the behavior of the latter sample in terms of the phase diagram (Fig. 1).

Sample G-82-119 Sn^+ is a clear combination of both superconducting and normal materials. Under microscopic examination the phases appear completely separated, with tall, columnar growths of Nb_6Sn_5 protruding from the smooth A15 background. Thus we can model the sample as regions of normal metal imbedded in a background of high-T_c Nb_3Sn. This picture is consistent with $R_s(T)$ shown in Fig. 5. The steep slope at T_c is due to the A15 phase, and the large residual resistance is the temperature-independent loss of the normal-metal regions. We have estimated the amount of normal material in the sample by means of optical examination, and the magnitude of the residual surface resistance, which should be proportional to the areal fraction of normal material, agrees with the loss we expected. By subtracting the residual surface resistance from R_s, (see Fig. 5) we get close agreement with the predicted losses for homogeneous A15 material.

Turning to the "single-phase" samples, G-81-68 Nb^+ and G-81-119 Nb^+, we note that, according to the phase diagram in Fig. 1, these samples should be single phase. By all available indications, (SEM, electron beam microprobe, and X-ray analysis), they appear to be uniform. However, broad transitions in the rf losses are clear indications of some kind of inhomogeneity. Similar conclusions have been drawn on the basis of heat capacity data[8] obtained with

similar samples. These results are inconsistent with the accepted Nb-Sn phase diagram.

To resolve this contradiction, a *modified phase diagram* has been proposed. This is shown in Fig. 7, and again the samples have been marked on it. The single-phase A15 region is much narrower with the left phase boundary considerably shifted towards the right. Furthermore, the free energies of the BCC and A15 phases are apparently such that the phases find it difficult to separate physically, and the inhomogeneities are so fine-scaled that SEM, microprobe and X-rays fail to detect them. We suggest that metastable A15 with varying amounts of Sn (i.e. from 18-25 at.%) result, giving a continuous spread in T_c's. This would account for the broad transitions observed in Figs. 4 and 5 for G-82-68 Nb-rich and G-82-119 Nb-rich.

B. Phase-Locking

Given the new phase diagram, the prospects for making single-phase A15 material are much more restrictive. Adjusting the evaporation rates of the Nb and Sn sources to realize the narrower A15 region may be possible but depends on exactly how wide the single-phase region actually is. In our depostion scheme there also is a residual phase spread of ~ .2% across the sample's width. Fortunately, however, the following "trick" may allow us to overcome these difficulties.

D.A. Rudman of our group has studied the Sn re-evaporation process which was mentioned earlier.[9] He finds that Nb-Sn which is deposited at temperatures above ~ 850°C in the two-phase (A15 + Nb_6Sn_5) region of the phase diagram will reject the Nb_6Sn_5 phase until its Sn concentration reaches the phase boundary. At this point the re-evaporation stops, and the material "locks" in composition to the phase boundary which still appears to be at 25%

Sn, i.e., Nb_3Sn. While the detailed reason for this phenomenon is not known, it has considerable potential for practical applications.

Figure 8 is an example of this phase-locking. Two rows of ten "1/4-inch square" Nb-Sn samples were prepared under identical conditions in the same evaporator run except for the substrate temperature. In the particular evaporation configuration used, the Sn concentration is expected to increase linearly with position in the direction of the rows. The Sn concentration of each sample was measured by electron beam microprobe and plotted as a function of sample position in Fig. 8. In the control row of samples, made at 650°C, the Sn concentration varies linearly with position as expected. The phase boundary is marked visibly in the samples by the presence of large "snow-cone"-shaped grains that rise out of the film, giving a visually frosty appearance. Samples in the 880°C row have similar compositions below the A15 phase boundary, but along the rest of the row remain locked to that concentration with no evidence of the Nb_6Sn_5 phase.

We should note that this "phase-locking" phenomenon is very sensitive to temperature. If the substrate is poorly anchored to the holder so that its temperature is lower than expected or simply not uniform, then the samples will be two-phased. What is known to work on small substrates is not so easy to apply to the larger ones of interest in our RF studies. Achieving good thermal control of the substrates continues to be the major stumbling block in applying this "phase locking" technique to making single-phase A15 samples for rf measurements or application. With the larger sample geometries used in our rf studies, a constant temperature is more difficult to obtain.

C. Recent Results

Our most recent emphasis has been an attempt to apply the "phase-locking" technique to making rf samples. As emphasized above this requires a substrate holder which will keep the substrates uniform heated and thermally anchored. The substrate holder used to make samples G-82-68 and G-82-119 clearly did not fully meet these needs. The substrates were much cooler than indicated by the thermocouple inside the holder, because both runs produced a two-phase (A15 + Nb_6Sn_5) sample. If the substrates were at the thermocouple temperature (listed as nominal T_s in Table I), then according to the phase diagram (Fig. 7) G-82-68 Sn^+ at 910°C would be in the phase-locking region, and above that at 980°C would be G-82-119 Sn^+ in the Nb_3Sn and liquid region. Neither sample should have any of the Nb_6Sn_5 phase. We concluded that the problem continued to lie in the design of the substrate holder. The substrates were tightly clamped to the holder only at the ends, leaving the middle region where the sample was deposited free. The substrate material, sapphire, has a larger coefficient of expansion than the niobium holder. At evaporation temperatures of ~ 900°C, the substrate expands more, and, since its ends are fixed, must bow out in the middle and away from the holder. To apply "phase-locking" then, it is necessary to design a substrate holder which will press the substrate along its entire length.

Figure 2(c) shows our Mark III substrate holder design. Two rf samples and three 1/4-inch square samples (for material's diagnostics) can be prepared in each run. Temperature is measured by a thermocouple placed inside the Nb backing plate. The rf substrates are pressed to the flat backing plate along their entire length to prevent bowing. This posed a problem in alignment because of the small dimensions involved (the clips cover ~ 10 mils along each edge of the 2 mm wide substrate), but by making the clips ~ 100 mils

thick we could design them to be self-aligning. The drawback to "thicker clips" is that they produce some shadowing of the evaporation sources on the substrates, giving regions along the sample edge that are pure Sn or pure Nb. As discussed below we have found that photolithography techniques can be used to mask off the center portion of the sample, permitting removal of the edges by either chemical, plasma, or reactive ion beam etching.

Our first clips were made from TZM, an alloy of molybdenum with tantalum and zirconium, which was advertised as having the desirable high-temperature stiffness of molybdenum, but unlike molybdenum was easily machined. In trying to use our TZM clips we could not consistently make whole samples, because the sapphire substrates kept breaking. Chipping and breakage of the substrate along the edges underneath the overhang of the clips indicated that the clips weren't machined smoothly enough. A material that was easier to work with had to be found.

Niobium has proven to be a satisfactory choice. It is softer and (in this geometry) springier than TZM, thus it has more give. In the meantime we had made one more modification to the substrate holder. Checking the flatness of the backing plate, we found that it bowed in ~ 7 μ from the edges to the center. By polishing the plate to an optical flat this problem has been eliminated. These modifications were successfully tested in run G-83-67.

Samples G-83-67 were deposited at a rate of 22.7 Å/sec and are 0.75 μm thick. The substrate holder was at 900°C, as indicated by the thermocouple. G-83-67 Nb-rich was a smooth uniform film with a 25.2 ± 0.3% Sn composition, as measured by microprobe. The Sn-rich sample had some second phase spots, but they were fewer in number and further apart, than on samples made with the previous substrate holders. Finally, we observed that both samples had borders of pure Nb and Sn that we attributed to shadowing of the sources.

Temperature control was improved by the new substrate holder. We had two means of evaluating this. One is visual examination. At the temperatures in question, metals are glowing red, and slight temperature variations are easily detected. By comparing the color of the freshly deposited films from G-83-67 with those from previous runs, the samples looked hotter (and thus closer to the thermocouple's reading) and more uniform in temperature. Of course, a more definitive temperature test is the presence of phase-locking. Unfortunately, its absence is not conclusive. For the latter conclusion more work is necessary to calibrate the relative evaporation rates of the sources with the composition of deposited material. At any rate, the existance of fewer second phase spots in the Sn-rich sample shows that we are moving in th right direction.

We measured the rf losses of the Nb-rich sample; the result is shown i Fig. 6. There are two very sharp transitions: one, at 17.8K is the full T_c of the A15, Nb_3Sn; and the other at 6-8K is probably due to the Nb border where the Sn source would have been shadowed. We don't see the Sn border, since the T_c of Sn at 3.85 K is below the lowest temperature measured. It is encouraging that we should see such a sharp transition associated with the A15 material in a sample with no Nb_6Sn_5 phase.

We used photolithography techniques to remove the border regions and measured the rf losses again. Results are also plotted in Fig. 6. The lower transition has disappeared except for two small bumps at 6 K and 8 K, confirming that its cause was indeed Nb (T_c = 9 K) at the boundaries. To date this is our closest approach to theory. Also, this is the first time we have seen a non-zero slope for the $R_s(T)$ curve at our lowest temperatures, indicating that we have to go to lower temperatures to reach a lower residual surface resistance. This result is also our best effort so far, and suggests

that some or all of our residual surface resistance (see earlier reports for a discussion of this issue) may be due to disordered material at the edges of our sample.

D. Normal-State Losses

Finally, as a check of the validity of our rf measurement and a further materials diagnostic we have studied the normal-state surface resistance of these samples by comparing the value we get from our rf measurement with a theoretically determined value. To obtain the latter we need to know the electromagnetic fields at the sample - a complicated problem due to the boundary conditions of the cylindrically-symmetric fields at the rectangular cross-section of the sample.

The simplest situation occurs when the fields are highly perturbed with the electric field lines bent to conform to the sample's perimeter instead of a circular cross section. In this case, a good model of our samples is a metallic plane of finite thickness which is placed in a uniform magnetic field parallel to its surface. Using electromagnetic theory and assuming a classical skin depth we calculate the surface resistance to be:

$$R_s = \sqrt{\frac{\mu_o \omega}{2\sigma}} \; \frac{e^{d/\delta} - e^{-d/\delta} - 2\sin d/\delta}{e^{d/\delta} + e^{-d/\delta} + 2\cos d/\delta}$$

where σ = conductivity of metal

ω = frequency of applied field

d = thickness of film

$\delta = \sqrt{\frac{2}{\mu_o \omega \sigma}}$ = skin depth.

A "universal" curve of R_s vs d/δ is plotted in Fig. 9 along with our

experimental data. The latter is determined by our rf loss measurement and a dc measurement of ρ just above T_c. (From ρ we can calculate δ, and d is known from the evaporation rates.) Some earlier results with the elemental superconductors, Nb and Sn, are included in Fig. 9 which show good agreement between the theory and experiment.

The Nb_3Sn points, however, lie in a line with values of R_s that are ~ 200 times greater than predicted. This systematic error indicates that the model is too simple for Nb_3Sn in its normal state. Thus, the configuration of the fields at the sample is more complicated. We assume that our Nb_3Sn samples for which $d/\delta < 1$ are more transparent to the cavity's fields. This results in larger $\vec{E}$-fields inside the sample, and accounts for the greater losses measured. By modifying our theoretical model for samples with $d/\delta > 1$, we hope to verify the normal-state losses for all our materials. Note that this problem does not arise when the sample is superconducting. In this case the superconducting penetration depth $\lambda < d$ plays the role of the skin depth. Hence, our determination of the superconducting surface resistance of Nb_3Sn is not affected.

CONCLUDING OBSERVATIONS

As we have shown, the most promising method for preparing homogeneous A15 material is to apply the phase-locking technique. The great sensitivity of this procedure to substrate temperature, however, requires good control of this parameter. Designing a substrate holder to be in good thermal contact with the substrates is critical in attaining this result. Both the improved temperature control and the closer approach of $R_s(T)$ to the theory by samples made with the succeeding generations of substrate holders, reflect our

progress in solving this problem. Based on our results to date, we believe the prognosis for achieving good rf properties in Nb_3Sn films is favorable. Fortunately, this aspect of our work is continuing under the National Science Foundation support.

REFERENCES

1. D. Birk, G.J. Dick, W.A. Little, J.E. Mercereau, and D.J. Scalapino, Appl. Phys. Lett. 32, 466 (1978).
2. S.A. Reible, 1982 Proc. of Ultrasonics Symp. (IEEE, New York, 1982), Vol. I, pp. 190-201.
3. W.H. Henkels and C.J. Kircher, IEEE Trans. Magn. MAG-13, No. 1, 63 (1977).
4. RF Properties of Superconducting A15 Compounds, Final Technical Report, M. R. Beasley and H. A. Schwettman, W. W. Hansen Laboratories, G. L. Report No.,
5. RF Properties of Superconducting A15 Compounds, Final Technical Report, M. R. Beasley and H. A. Schwettman, W. W. Hansen Laboratories, G. L. Report No. 3602, July 1983.
6. L.H. Allen, M.R. Beasley, R.H. Hammond, and J.P. Turneaure, IEEE Trans. Magn. MAG-19, No. 3, 1003 (1983).
7. J.P. Charlesworth, I. MacPhail, and P.E. Madsen, J. Mat. Sci. 5, 580 (1970).
9. F. Hellman, D.A. Rudman, R.H. Hammond, and T.H. Geballe, Bull. Am. Phys. Soc. 28, 262 (1983).
9. D.A. Rudman, F. Hellman, R.H. Hammond, and M.R. Beasley, to appear in J. Appl. Phys.

TABLE I. SAMPLES FOR RF STUDIES

Sample Number	%Sn	Thermcouple T_s (°C)	Deposition Rates (Å/sec)	T_c^{rf} (K)	d (μm)	ρ ($\mu\Omega$-cm)	d/δ	Resistance Ratio	Substrate Holder	Comments
G-80-122	24.3±.1	700	30.7	17.5±.1	1.0	8.6	.64	1.9	Mark I	Believe thermocouple read substrate's temperature
G-82-68		910-920	24.2	17.7±.1	.79	25	.30	3.7	Mark II	Thermocouple read holder's temperature. Est. substrate ∿100° colder
G-82-68	26.7±.5*	910-920	24.2	--	.79	14	.41	6.7	Mark II	Thermocouple read holder's temperature. Est. substrate ∿100° colder
G-82-119 Nb-rich	24.7±.4	980	24.0	17.8±.1	.75	19	.32	4.2	Mark II	Thermocouple read holder's temp. Est. substrate ∿150° colder
G-82-119 Sn-rich	26.8±.4*	980	24.0	17.6±.1	.75	13	.39	6.4	Mark II	Thermocouple read holder's temp. Est. substrate ∿150°colder
G-83-67 Nb-rich	25.2±.3	900	22.7	17.8±.1	.75	--	--	--	Mark III	Thermocouple read holder's temp. Est. substrate ∿50° colder

*inferred

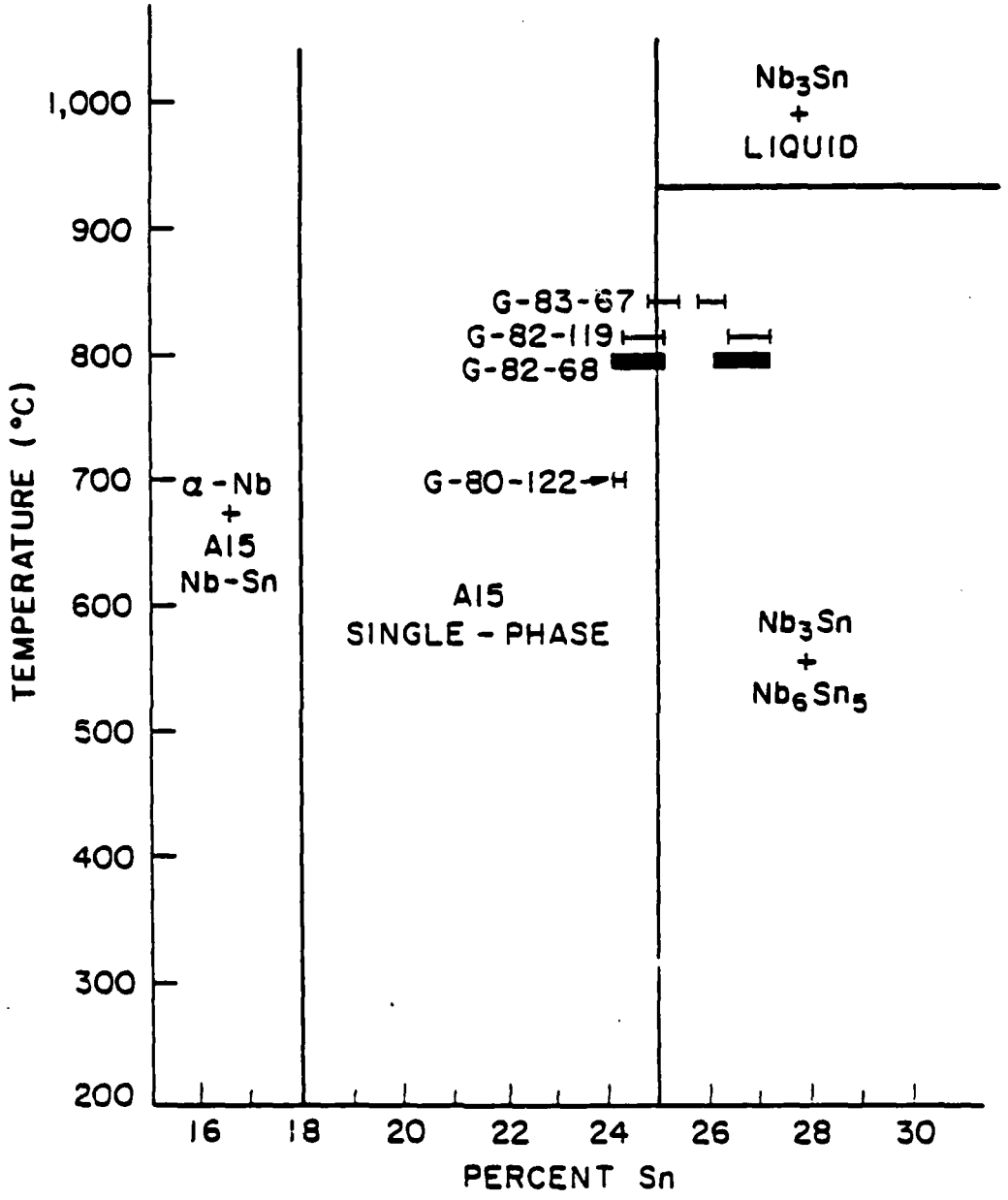

FIG. 1--The accepted phase diagram for Nb_3Sn. The samples we discuss are marked.

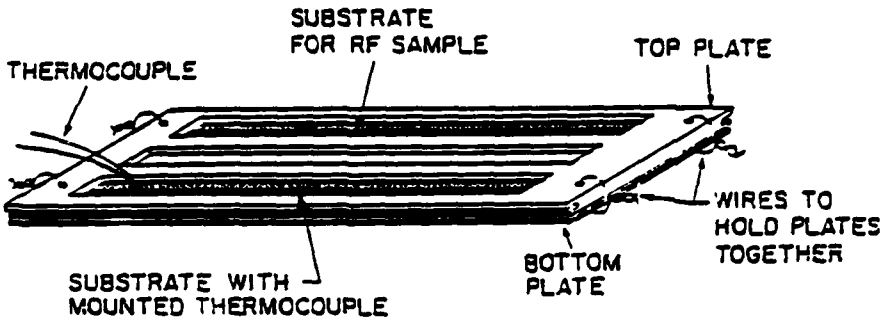

(a)

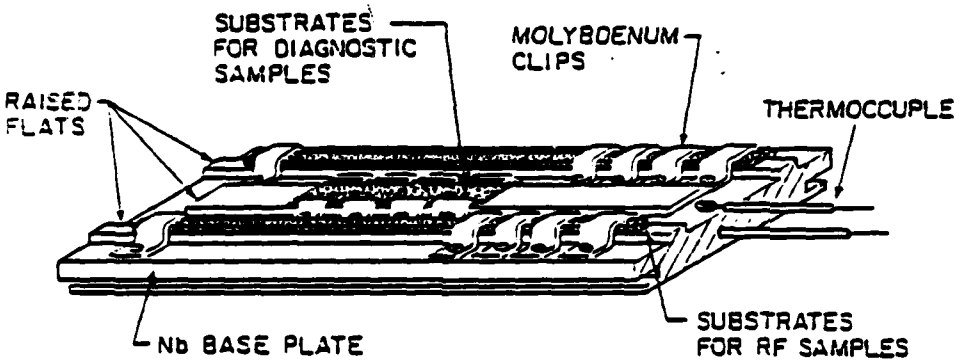

(b)

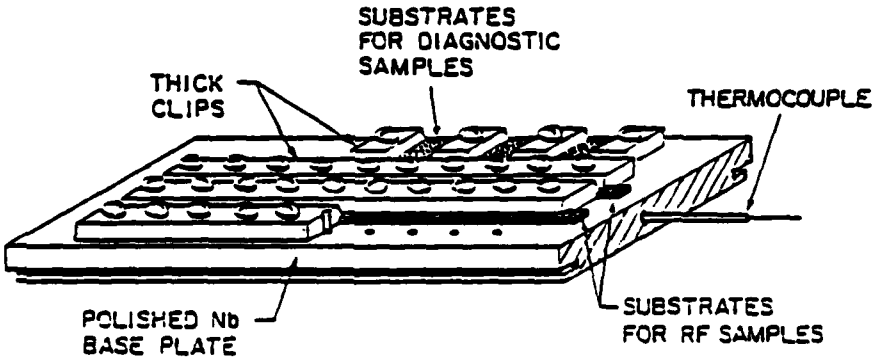

(c)

FIG. 2--The evolution of substrate holders;
(a) MARK I, (b) MARK II, (c) MARK III.

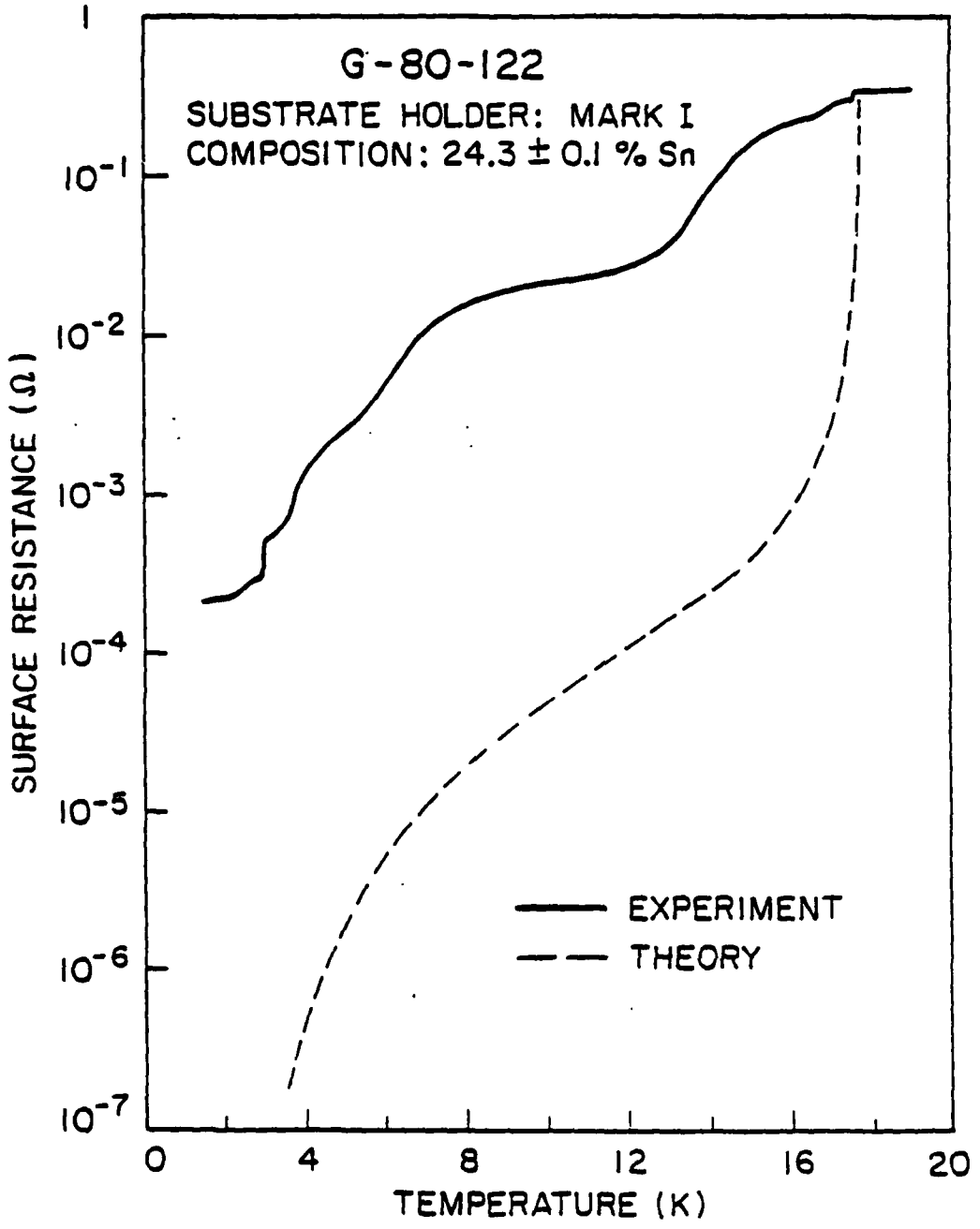
G-80-122
SUBSTRATE HOLDER: MARK I
COMPOSITION: 24.3 ± 0.1 % Sn
SURFACE RESISTANCE (Ω)
1
10-1
10-2
10-3
10-4
10-5
10-6
10-7
0
4
8
12
16
20
TEMPERATURE (K)
EXPERIMENT
THEORY

FIG. 3

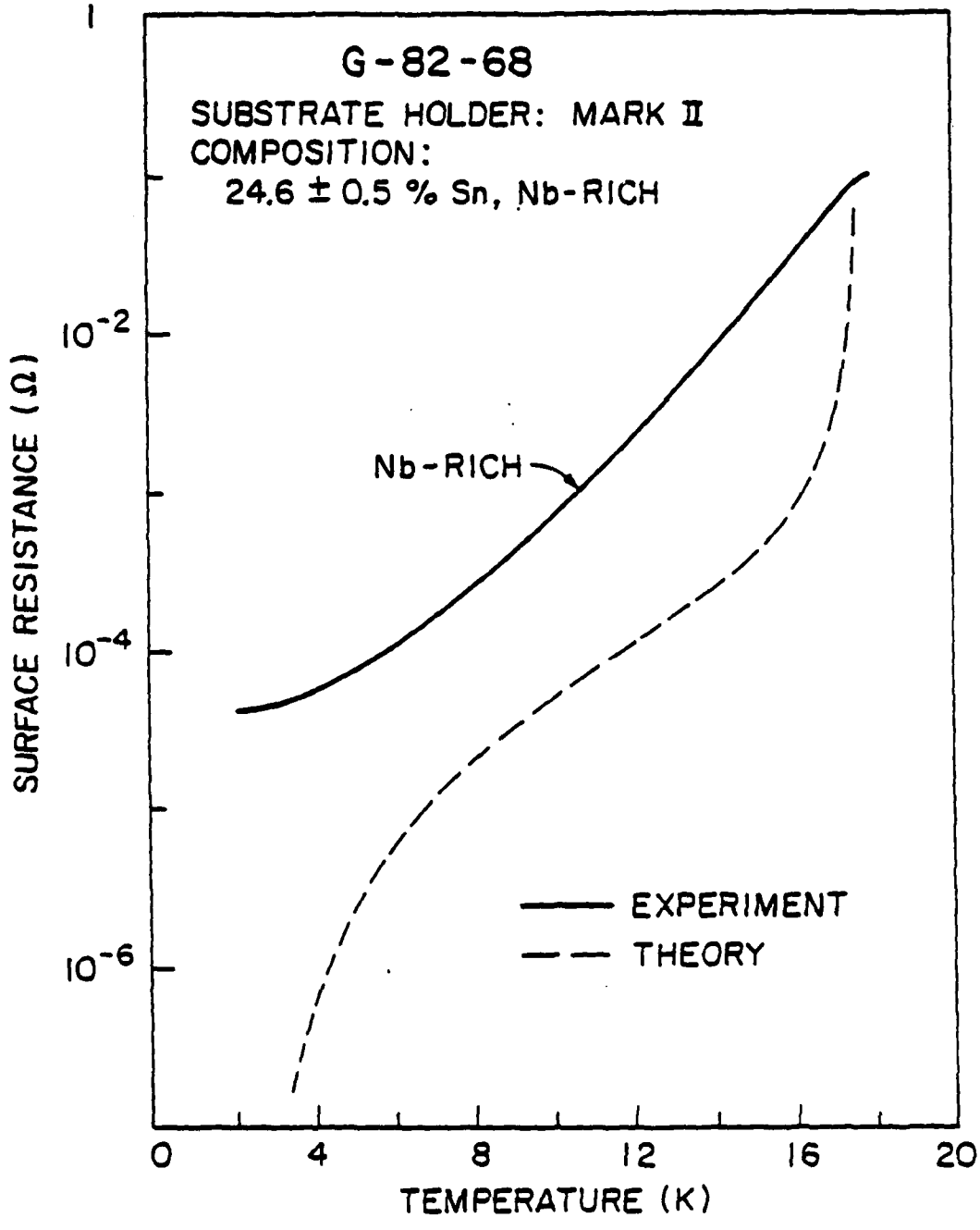
G-82-68
SUBSTRATE HOLDER: MARK II
COMPOSITION:
24.6 ± 0.5 % Sn, Nb-RICH
SURFACE RESISTANCE (Ω)
1
10^{-2}
10^{-4}
10^{-6}
Nb-RICH
EXPERIMENT
THEORY
0
4
8
12
16
20
TEMPERATURE (K)

FIG. 4

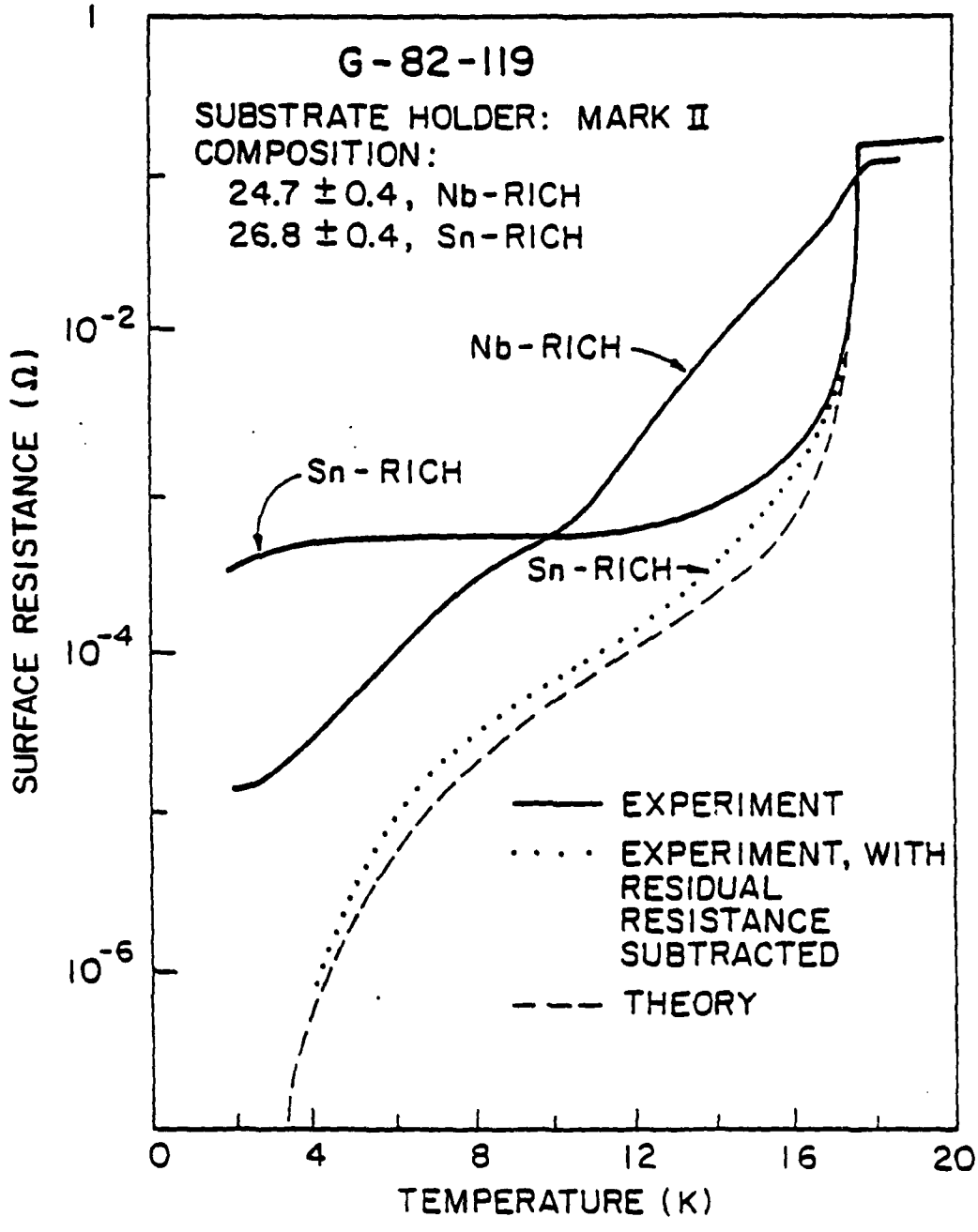
G-82-119
SUBSTRATE HOLDER: MARK II
COMPOSITION:
24.7 ± 0.4, Nb-RICH
26.8 ± 0.4, Sn-RICH
Nb-RICH
Sn-RICH
Sn-RICH
EXPERIMENT
EXPERIMENT, WITH RESIDUAL RESISTANCE SUBTRACTED
THEORY
SURFACE RESISTANCE (Ω)
1
10^{-2}
10^{-4}
10^{-6}
0
4
8
12
16
20
TEMPERATURE (K)

FIG. 5

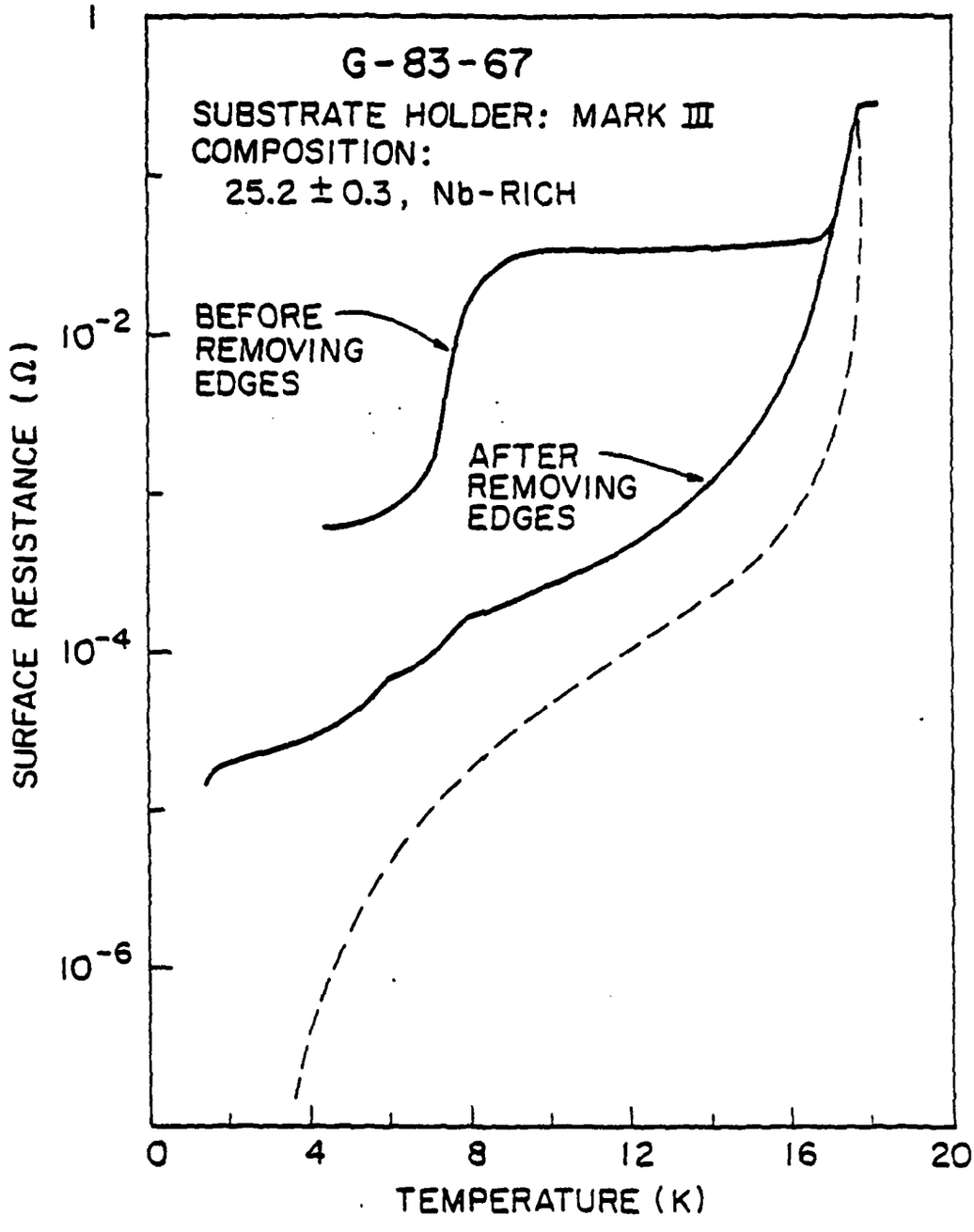
G-83-67
SUBSTRATE HOLDER: MARK III
COMPOSITION:
25.2 ± 0.3, Nb-RICH
BEFORE REMOVING EDGES
AFTER REMOVING EDGES
SURFACE RESISTANCE (Ω)
1
10^{-2}
10^{-4}
10^{-6}
0
4
8
12
16
20
TEMPERATURE (K)

FIG. 6

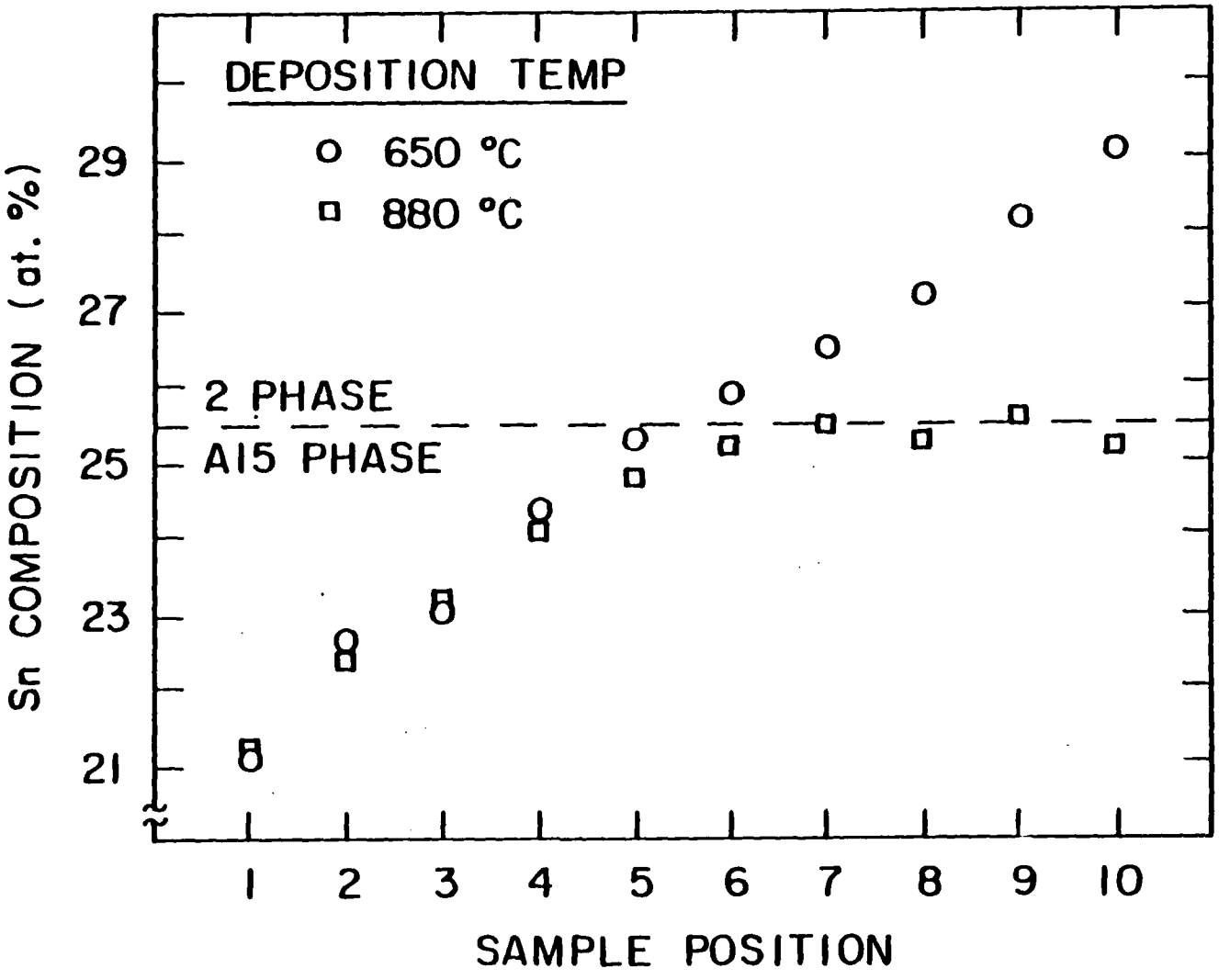

FIG. 8--The variation of sample composition with substrate position shows "phase-locking" of Sn composition to stoichiometry for a sufficiently high deposition temperature. (From Ref. 7).

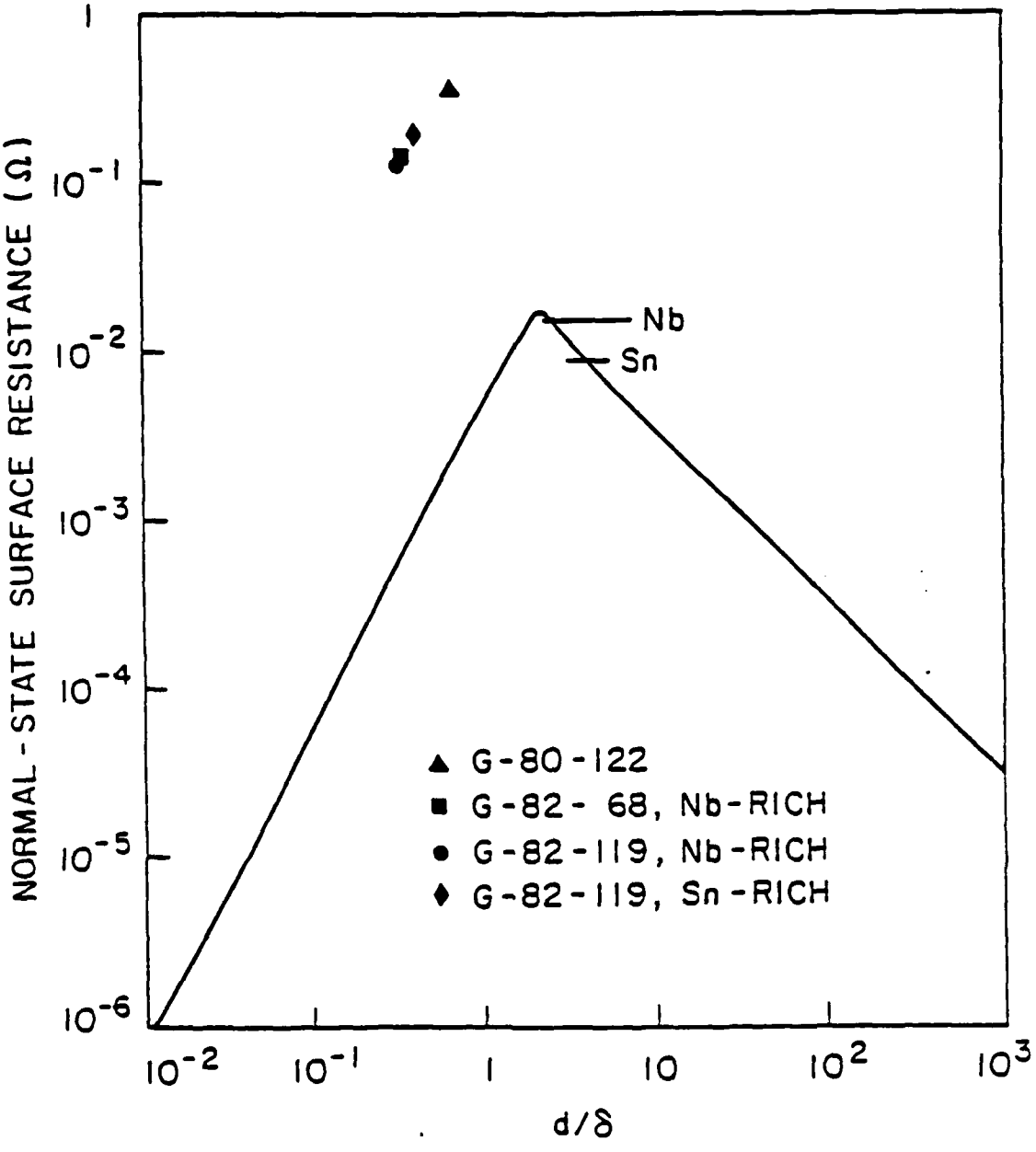

FIG. 9--The dependence of normal state surface resistance on d/δ. The curve is derived from a calculation for a conducting plane of finite thickness in a uniform magnetic field. The data points are determined by the rf surface resistance and a dc measurement of ρ above T_c. The Nb_3Sn data is systematically greater than predicted.